

Exploring the quantum vacuum with cylinders

F.C. Lombardo, F D Mazzitelli, and P.I. Villar

Departamento de Física J.J. Giambiagi, Facultad de Ciencias Exactas y Naturales,
Universidad de Buenos Aires, Ciudad Universitaria, Pabellón 1, 1428 Buenos Aires,
Argentina

E-mail: lombardo@df.uba.ar, fmazzi@df.uba.ar, paula@df.uba.ar

Abstract. We review recent work on the Casimir interaction energy between cylindrical shells. We include proposals for future experiments involving cylinders, such as a null experiment using quasi-concentric cylinders, a cylinder in front a conducting plate, and a cylindrical version of the rack and pinion powered by Casimir lateral force. We also present an exact formula for the theoretical evaluation of the vacuum interaction energy between eccentric cylindrical shells, and describe improved analytical and numerical evaluations for the particular case of concentric cylinders.

PACS numbers: 12.20.-m, 03.70.+k, 04.80.Cc

Keywords: Casimir effect, quantum vacuum, cavity QED

Submitted to: *J. Phys. A: Math. Gen.*

1. Introduction

Up to now, most experiments aiming at a measurement of the Casimir force have been performed with parallel plates [1], or with a sphere in front of a plane [2]. The parallel plates configuration has a stronger signal, but the main experimental difficulty is to achieve parallelism between the plates. This problem is of course not present in the case of a sphere in front of a plane, but its drawback is that the force is several orders of magnitude smaller. On the theoretical side, the evaluation of the electromagnetic force for this configuration is still an open problem [3].

In this paper we will consider different configurations that involve cylindrical surfaces. As we will see, these configurations have both experimental and theoretical interest. In the next Section we will describe some promising experimental proposals. In Section 3 we will present an exact formula for the Casimir interaction energy between two eccentric cylindrical shells, and we will show that particular known formulas, such as the corresponding to a cylinder in front of a plane or the one of concentric cylinders, are included therein. Finally, for the particular case of concentric cylinders, in Section

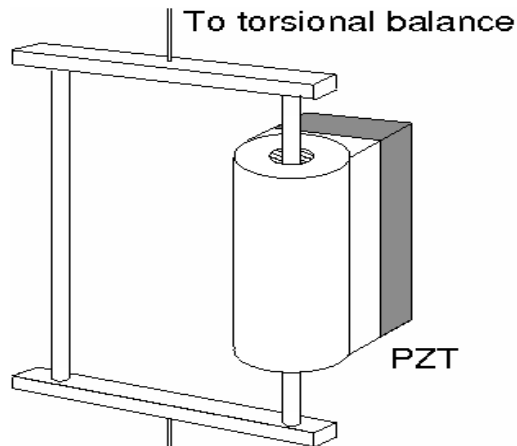


Figure 1. Experimental setup for detecting Casimir forces using quasi-concentric cylinders. The inner cylinder is rigidly connected to a torsional balance and the signal to restore the concentric configuration is measured after a controlled displacement.

4 we will present a new analytic result beyond the Proximity Force Approximation (PFA), and an improved numerical method to evaluate the interaction energy at small distances.

2. Experimental proposals

We discuss possible experimental arrangements for measuring the Casimir force between cylinders. As it was reported in the last years, cylindrical shells provide a new and promising arena to study Casimir interactions [4, 5].

2.1. A null experiment

Let us first consider the case of two eccentric cylindrical shells, in an almost coaxial configuration. The concentric is an unstable equilibrium position, so one possibility is to repeat a microscopic version of the experiment described in [6] to test universal gravitation in the cm range, with a small torsional balance mounted on the ends of the internal cylinder. In this case the unstable force could be evidenced by intentionally creating a controlled eccentricity and measuring the feedback force required to bring the internal cylinder to zero eccentricity, as depicted in Fig. 1 [4].

This configuration has some advantages over the parallel plates geometry. If there is no residual charge in the inner cylinder, the system remains neutral and screened by the external one from background noise sources, and from residual charges in the outer cylinder. When the inner cylinder has a residual charge, there will be a small potential difference between the cylinders, and the coaxial configuration will be electrostatically unstable. The electrostatic instability can be avoided by putting the cylinders in contact, something ineluctable during the preliminary stages of parallelization. Then the residual charge of the inner cylinder will flow to the hollow cylinder, apart from a residual charge

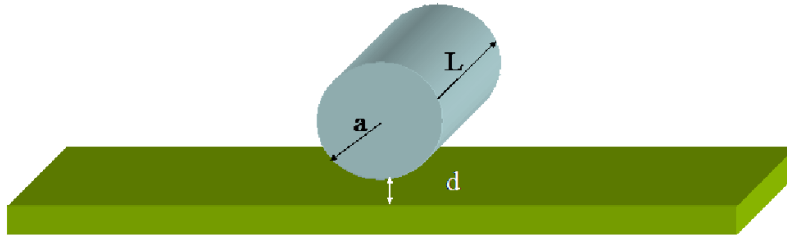


Figure 2. Cylindrical shell in front of a conducting plane. Using PFA one can show that the scaling of the Casimir force with distance is $\propto d^{-7/2}$ [4], which is intermediate between the plane-spherical ($\propto d^{-3}$) and the parallel plate configuration ($\propto d^{-4}$). This configuration is also intermediate for the absolute value of the force signal for typical values of the geometrical parameters.

due to the imperfections and finite length of the cylinders. This residual charge will be smaller than for other geometries, as the same discharging procedure does not work in the other configurations (the efficiency of this procedure could be affected by the fact that repeated contact between the cylindrical shells may result in a degradation of the surfaces, as for instance an increased rugosity).

The electrostatic instability could also be exploited to improve the parallelism between cylinders. One could apply a time-dependent potential between the cylinders and measure the force, as in the experiments to test the inverse-square Coulomb law. Parallelism and concentricity would be maximum for a minimum value of the force. Moreover, the expected gravitational force is obviously null, this being an advantage if one looks for intrinsically short-range extra-gravitational forces [7].

2.2. A cylinder in front of a conducting plane

Another possibility, which in principle is much more appealing from the experimental point of view, is to consider the configuration of a cylinder in front of a plane. The cylinder-plane configuration of Fig. 2 is a compromise between the different drawbacks and advantages of the parallel-plates and the sphere-plate configurations. While this geometry offers a simpler way to control the parallelism with respect to the parallel plate case, at the same time gives rise to considerable force signal which requires the study of the force at larger distances. Not only can the study of the cylindrical-plane configuration provide insights into the thermal contribution to the Casimir force arising at any finite temperature, but also into the validity of the PFA. This is because, as the signal is stronger than in the sphere plane configuration, one can envisage sufficiently precise measurements at larger distances. This experiment is in progress [5, 8].

2.3. Cylindrical rack and pinion

Another interesting configuration is a cylindrical version of the Casimir “rack and pinion” proposed in Ref.[9], in which the rack is a corrugated cylindrical shell that

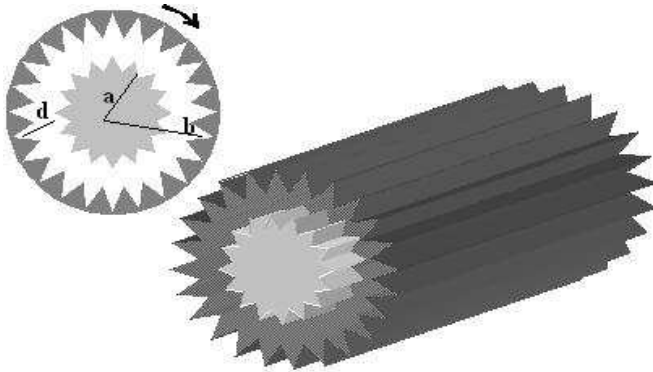


Figure 3. Cylindrical version of the Casimir "rack and pinion". Rotation of the outer cylinder induces a torque on the inner corrugated cylinder due to the lateral Casimir force.

encloses the pinion, instead of a corrugated plane (see Fig. 3). In this case, the cylindrical geometry is of interest for the opposite reason than before: while reaching parallelism may be more complicated than from the plane rack, the torque will be enhanced by a geometric factor, and therefore could be more useful to generate the motion of the pinion. Indeed, the interaction energy per unit area between sinusoidally corrugated plane surfaces is given by [9]

$$E_{pp} = \frac{\hbar c h^2}{d^5} \cos\left(\frac{2\pi x}{\lambda}\right) J\left(\frac{d}{\lambda}\right), \quad (1)$$

where d is the mean distance between the plates, h is the amplitude of the corrugations and x is the lateral displacement. We will not need the explicit form of the function J .

The interaction energy for the plane and for the cylindrical rack and pinion can be easily computed using the PFA. In the first case it is given by

$$E_{prp} = \hbar c h^2 \cos\left(\frac{2\pi x}{\lambda}\right) L a \int d\theta \frac{J\left(\frac{d(\theta)}{\lambda}\right)}{d^5(\theta)}, \quad (2)$$

where a and L are the radius and length of the cylinder, respectively, and $d(\theta) = d + a(1 - \cos\theta)$.

For the cylindrical case we have, instead, $E_{crp} = 2\pi a L E_{pp}$. This simple result is valid when the radii of the outer (b) and the inner (a) cylinders satisfy $a \simeq b \gg d$. Note that this configuration maximizes the superposition between the two surfaces, and therefore a uniform rotation of the external shell will produce a torque on the pinion much larger than the one produced by a plane rack moving with uniform velocity.

The ratio of the forces can be easily estimated from the ratio of the interaction energies. Assuming that $J\left(\frac{d(\theta)}{\lambda}\right)$ is a smooth function, and that the integral in Eq. (2) is dominated by $\theta \approx 0$, we obtain $F_{crp}/F_{prp} \gtrsim \sqrt{a/d} \gg 1$.

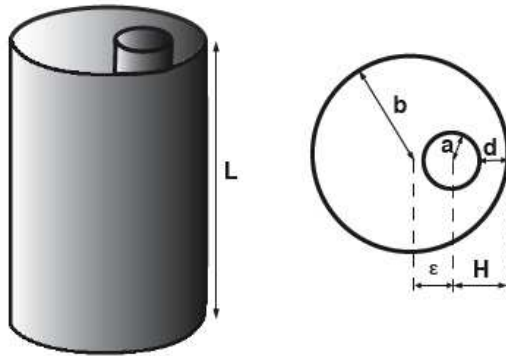


Figure 4. Geometrical configuration for the eccentric cylinders. Two perfectly conducting cylinders of radii $a < b$, length L , and eccentricity ϵ interacts via the Casimir force.

3. The exact formula for eccentric cylinders

The evaluation of the Casimir interaction energy between eccentric cylindrical shells (Fig. 4) has been initially performed using the PFA in Ref.[4], where the force between a cylinder and a plate has also been computed and discussed for the first time using the same approximation. However, it is possible to go beyond the PFA, and find an exact formula for the interaction energy [10, 11]. This can be done using a mode by mode summation technique combined with the argument theorem.

We start by expressing the Casimir energy as $E = (\hbar/2) \sum_p (\omega_p - \tilde{\omega}_p)$, where ω_p are the eigenfrequencies of the electromagnetic field satisfying perfect conductor boundary conditions on the cylindrical surfaces, and $\tilde{\omega}_p$ are the corresponding ones to the reference vacuum (cylinders at infinite separation). In cylindrical coordinates, the eigenmodes are $h_{n,k_z} = R_n(r, \theta) \exp[-i(\omega_{n,k_z} t - k_z z)]$, where $\omega_p = \omega_{n,k_z} = \sqrt{k_z^2 + \lambda_n^2}$, and R_n (λ_n) are the eigenfunctions (eigenvalues) of the 2D Helmholtz equation. Using the argument theorem the sum over eigenmodes can be written as an integral over the complex plane, with an exponential cutoff for regularization. In order to determine the part of the energy that depends on the separation between the two cylinders it is convenient to subtract the self-energies of the two isolated cylinders, $E_{12}(a, b, \epsilon) = E - E_1(a) - E_1(b)$. Then the divergencies in E are cancelled out by those ones in $E_1(a)$ and $E_1(b)$, and the final result for the interaction energy is

$$E_{12}(a, b, \epsilon) = \frac{\hbar c L}{4\pi} \int_0^\infty dy y \log M(iy). \quad (3)$$

Here $M = (F/F_\infty)/[(F_1(\infty)/F_1(a)) (F_1(\infty)/F_1(b))]$. The function F is analytic and vanishes at all the eigenvalues λ_n (F_∞ , at $\tilde{\lambda}_n$), and, similarly, F_1 vanishes for all eigenvalues of the isolated cylinders. The function M is the ratio between a function corresponding to the actual geometrical configuration and the one with the conducting cylinders far away from each other. It is convenient to subtract a configuration of two cylinders with very large and very different radii, while keeping the same eccentricity of

the original configuration. Eq. (3) is valid for two perfect conductors of any shape, as long as there is translational invariance along the z axis.

The solution of the Helmholtz equation in the annulus region between eccentric cylinders has been considered in the framework of classical electrodynamics and fluid dynamics. The eigenfrequencies for Dirichlet boundary conditions (TM modes) and for Neumann boundary conditions (TE modes) are given by the zeros of the determinants of the non-diagonal matrices

$$\begin{aligned} Q_{mn}^{\text{TM}} &= [J_n(\lambda a)N_m(\lambda b) - J_m(\lambda b)N_n(\lambda a)] J_{n-m}(\lambda \epsilon), \\ Q_{mn}^{\text{TE}} &= [J'_n(\lambda a)N'_m(\lambda b) - J'_m(\lambda b)N'_n(\lambda a)] J_{n-m}(\lambda \epsilon), \end{aligned}$$

where J_n and N_n are Bessel functions of the first kind. The function M can be written as $M = M^{\text{TE}}M^{\text{TM}}$, where M^{TM} is built with

$$\begin{aligned} F^{\text{TM}} &= \det [Q^{\text{TM}}(a, b, \epsilon)Q^{\text{TM}}(b, R, 0)] \prod_n J_n(\lambda a), \\ F_1^{\text{TM}}(a) &= \det [Q^{\text{TM}}(a, R, 0)] \prod_n J_n(\lambda a), \end{aligned} \quad (4)$$

and R is a very large radius. Similar expressions hold for M^{TE} .

The Casimir energy can be decomposed as a sum of TE and TM contributions

$$E_{12} = \frac{\hbar c L}{4\pi a^2} \int_0^\infty d\beta \beta \left[\log M^{\text{TE}} \left(\frac{i\beta}{a} \right) + \log M^{\text{TM}} \left(\frac{i\beta}{a} \right) \right] \quad (5)$$

with $M^{\text{TE, TM}} \left(\frac{i\beta}{a} \right) = \det [\delta_{np} - A_{np}^{\text{TE, TM}}]$. The non-diagonal matrices A_{np}^{TE} and A_{np}^{TM} are

$$\begin{aligned} A_{np}^{\text{TM}} &= \frac{I_n(\beta)}{K_n(\beta)} \sum_m \frac{K_m(\alpha\beta)}{I_m(\alpha\beta)} I_{m-n}(\beta\delta) I_{m-p}(\beta\delta), \\ A_{np}^{\text{TE}} &= \frac{I'_n(\beta)}{K'_n(\beta)} \sum_m \frac{K'_m(\alpha\beta)}{I'_m(\alpha\beta)} I_{m-n}(\beta\delta) I_{m-p}(\beta\delta). \end{aligned}$$

Here I_n and K_n are modified Bessel functions of the first kind, $\alpha = b/a$ and $\delta = \epsilon/a$. The determinants are taken with respect to the integer indices $n, p = -\infty, \dots, \infty$, and the integer index m runs from $-\infty$ to ∞ . Eq.(5) is the exact formula for the interaction Casimir energy between eccentric cylinders.

This expression is rather complex to evaluate numerically, since each term in the infinite matrix is a series involving Bessel functions. However, we have been able to numerically evaluate the exact Casimir interaction energy between eccentric cylinders as a function of α for different values of the eccentricity [11]. We have calculated this energy as a function of α for values that interpolate between the PFA (small α) values, and the asymptotic behavior for large α (see Fig. 5). The numerical convergence is better as α increases, while bigger matrices and more terms in each matrix element are needed as α gets closer to 1.

An interesting property of the exact formula is that reproduces the exact Casimir interaction energy for the cylinder-plane configuration as a limiting case. Indeed, the eccentric cylinder configuration tends to the cylinder-plane configuration for large values

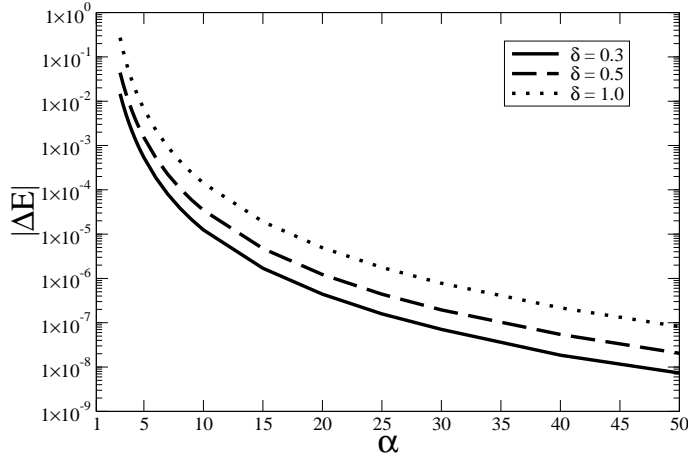


Figure 5. Exact Casimir interaction energy difference $|\Delta E|$ between the eccentric and concentric configurations as a function of $\alpha = b/a$ for different values of $\delta = \epsilon/a$. Energies are measured in units of $L/4\pi a^2$.

of both the eccentricity ϵ and the radius b of the outer cylinder, keeping the radius a of the inner cylinder and the distance d between the cylinders fixed. Using the addition theorem and uniform expansions for Bessel functions it can be proved that, for $x \gg h$,

$$\sum_m \frac{K_m(x+h)}{I_m(x+h)} I_{n-m}(x) I_{p-m}(x) \approx K_{n+p}(2h),$$

$$\sum_m \frac{K'_m(x+h)}{I'_m(x+h)} I_{n-m}(x) I_{p-m}(x) \approx -K_{n+p}(2h).$$

Using these equations (with $x \equiv \beta\epsilon/a$ and $h \equiv \beta H/a$) in our exact formula we find

$$A_{np}^{\text{TM},c-p} = \frac{I_n(\beta)}{K_n(\beta)} K_{n+p}(2\beta H/a),$$

$$A_{np}^{\text{TE},c-p} = -\frac{I'_n(\beta)}{K'_n(\beta)} K_{n+p}(2\beta H/a),$$

which is the known result for the Casimir energy in the cylinder-plane configuration [12].

4. Concentric cylinders: new analytic and numerical results

The exact formula for eccentric cylinders coincides, of course, with the known result for the Casimir energy for concentric cylinders ($\epsilon = 0$). Indeed, as $I_{n-m}(0) = \delta_{nm}$, in this particular case the matrices $A_{np}^{\text{TE},\text{TM}}$ become diagonal and the exact formula reduces to [13]:

$$E_{12}^{\text{cc}} = \frac{L}{4\pi a^2} \int_0^\infty d\beta \beta \ln M^{\text{cc}}(\beta), \quad (6)$$

where

$$M^{\text{cc}}(\beta) = \prod_n \left[1 - \frac{I_n(\beta)K_n(\alpha\beta)}{I_n(\alpha\beta)K_n(\beta)} \right] \left[1 - \frac{I'_n(\beta)K'_n(\alpha\beta)}{I'_n(\alpha\beta)K'_n(\beta)} \right]. \quad (7)$$

The first factor corresponds to Dirichlet (TM) modes and the second one to Neumann (TE) modes. The concentric-cylinders configuration is interesting from a theoretical point of view, since it can be used to test analytic and numerical methods. It also has potential implications for the physics of nanotubes [10, 14].

The short distance limit $\alpha - 1 \ll 1$ has already been analyzed for this case [13], and involves the summation over all values of n . As expected, the resulting value is equal to the one obtained via the proximity approximation, namely

$$E_{12,\text{PFA}}^{\text{cc}} = -\frac{\pi^3 L}{360a^2} \frac{1}{(\alpha - 1)^3}. \quad (8)$$

In the opposite limit ($\alpha \gg 1$) it is easy to prove that to leading order only the $n = 0$ term contributes to the interaction energy, and the energy decreases logarithmically with the ratio $\alpha = b/a$,

$$E_{12}^{\text{cc}} \approx -\frac{1.26L}{8\pi b^2 \ln \alpha}. \quad (9)$$

It is worth noticing that, while for small values of α both TM and TE modes contribute with the same weight to the interaction energy, the TM modes dominate in the large α limit.

4.1. Beyond proximity approximation: the next to next to leading order

In this Section we will compute analytic corrections to the PFA given in Eq.(8). Due to the simplicity of this configuration, we will be able to obtain not only the next to leading order, but also the next to next to leading contribution. In order to do that, we need the uniform expansion of the Bessel functions. For example, we write

$$\frac{K_n(n\alpha y)}{K_n(ny)} = \frac{\sqrt{1+y^2}}{\sqrt{1+\alpha^2 y^2}} \frac{(1 - \frac{u(t_\alpha)}{n})}{(1 - \frac{u(t_1)}{n})} e^{n[\eta(\alpha y) - \eta(y)]}, \quad (10)$$

where

$$\eta(y) = \sqrt{1+y^2} + \ln \frac{y}{1 + \sqrt{1+y^2}}; \quad u(t) = \frac{3t - 5t^3}{24}; \quad t_\alpha = \frac{1}{\sqrt{1+\alpha^2 y^2}}, \quad (11)$$

and similar expressions for the functions I_n .

With these expansions at hand, we can evaluate the the matrix M both for the TE and TM modes. After a long calculation, it is possible to show that the Casimir energy, beyond the proximity approximation can be written as

$$E_{12}^{\text{cc}} \approx -\frac{\pi^3 L}{360a^2(\alpha - 1)^3} \left\{ 1 + \frac{1}{2}(\alpha - 1) - \left(\frac{2}{\pi^2} + \frac{1}{10} \right) (\alpha - 1)^2 + \dots \right\}. \quad (12)$$

In the expression above, the first term inside the parenthesis corresponds to the proximity approximation contribution in Eq.(8), while the second and third terms are the first and second order corrections, respectively. It is important to stress here that both TM and TE modes contribute with the same weight to the energy up to the next to leading order, but it is not the case in the third term. There is a factor $1/\pi^2$ coming from the TM mode, and a factor $1/\pi^2 + 1/10$ corresponding to the TE one.

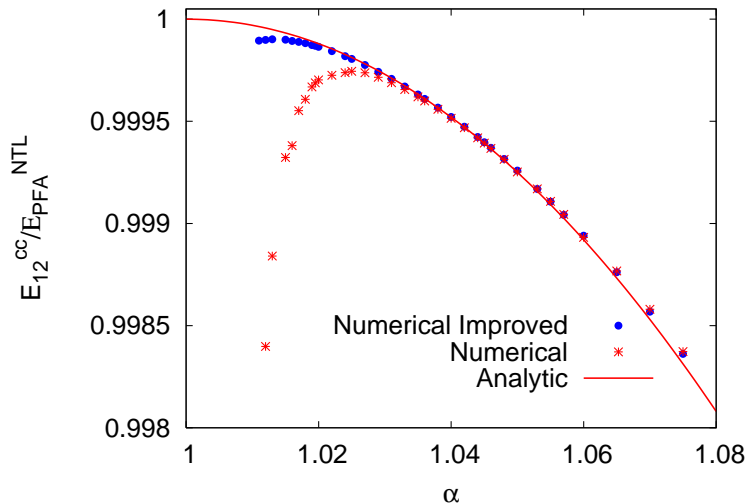


Figure 6. Ratio between the exact Casimir energy for concentric cylinders E_{12}^{cc} and the Casimir energy estimated using the PFA up to the next to leading order E_{PFA}^{NTL} , as a function of the parameter α . This is done for two different methods: the numerical (of slow convergence) and the numerical improved (subtraction method). Solid line indicates the analytic result from Eq.(12).

4.2. Improving the convergence of the numerical evaluation

Numerical calculations of the Casimir energy for α very close to one are really difficult since big number of terms have to be considered in the sums, and therefore convergence problems arise.

In order to perform a numerical evaluation of the Casimir energy for the concentric cylinder case, we will describe a subtraction method, in which we have used the proximity approximation value of the energy to improve numerics.

As a guiding example, let us consider the following sum:

$$z_M = \sum_{n=1}^M \frac{1}{n^{1.1}}. \quad (13)$$

The convergence of this sum as $M \rightarrow \infty$ is extremely slow, as the following numbers suggest: $z_{10^3} = 5.5728$, $z_{10^5} = 7.4222$ and $z_{\infty} = 10.5844$. About 10^{20} terms are needed to get an accuracy of 1%.

Then, we add and subtract the function $\int_1^M \frac{dx}{x^{1.1}}$, that reproduces the behaviour of the series when the exponent in the denominator is close to one. In this way,

$$z_M = z_M - \int_1^M \frac{dx}{x^{1.1}} + \int_1^M \frac{dx}{x^{1.1}} = D_M + \int_1^M \frac{dx}{x^{1.1}} \rightarrow D_{\infty} + 10. \quad (14)$$

The convergence of the new function D_M is notably faster as $D_{10} = 0.6234$ and $D_{1000} = 0.5847$, i.e. 1% accuracy is obtained with less than 10 terms.

In the case we are concerned here, we can add and subtract the interaction energy for concentric cylinders computed using the leading uniform asymptotic expansion for

the Bessel functions, up to first order in $\alpha - 1$:

$$\frac{K_n(n\alpha y)}{K_n(ny)} \frac{I_n(ny)}{I_n(n\alpha y)} \simeq e^{-2n(\alpha-1)\sqrt{1+y^2}}. \quad (15)$$

We denote by \tilde{E} the interaction energy obtained by inserting these expansions into Eq. (6). Now we write

$$E_{12}^{cc} = (E_{12}^{cc} - \tilde{E}) + \tilde{E}. \quad (16)$$

The last term in the above expression is easily written into an analytic expression, which contains the leading order of the Casimir energy. Meanwhile, the difference contained in the brackets in Eq. (16), has a faster convergence than the original sum and therefore, can be easily calculated numerically.

In this context, in Fig.6 we present both Casimir energy of the concentric cylinders for the direct numerical calculation (of slow convergence) and the alternative method mentioned above. In this figure we plot the ratio $E_{12}^{cc}/E_{PFA}^{NTL}$ where

$$E_{PFA}^{NTL} = -\frac{\pi^3 L}{360a^2(\alpha-1)^3} \left\{ 1 + \frac{1}{2}(\alpha-1) \right\}. \quad (17)$$

As can be seen, with this subtraction method it is possible to compute the exact energy for values of α much closer to 1, while the accuracy of the direct calculation is worse for $\alpha < 1.02$.

A similar method could in principle be applied to the eccentric cylinders or the cylinder-plane configurations, although in these cases the main difficulty is the analytic evaluation of the approximate energy to be added and subtracted.

5. Final remarks

In this paper we have described experimental proposals and theoretical aspects of the Casimir interaction energy between cylindrical shells. We have reviewed previous works on the subject, in which we obtained an exact formula for the interaction energy between eccentric cylinders [10, 11], and where we discussed the advantages of considering experiments involving cylinders [4, 5].

We have also presented some new results. In particular, we have shown that a cylindrical version of the non contact rack and pinion powered by the lateral Casimir force, proposed in Ref.[9], would have a larger torque because of a geometric enhancement.

From a theoretical point of view, we have found an analytic formula for the interaction energy between concentric cylinders beyond the PFA, including first and second order corrections. We have also presented a subtraction method useful to improve the convergence of the numerical calculations as the concentric surfaces get closer to each other. We hope to generalize these results to other geometries in future works.

Acknowledgments

This work has been supported by CONICET, UBA and ANPCyT, Argentina.

References

- [1] G. Bressi, G. Carugno, R. Onofrio, and G. Ruoso, *Phys. Rev. Lett.* **88**, 041804 (2002).
- [2] S.K. Lamoreaux, *Phys. Rev. Lett.* **78**, 5 (1997); U. Mohideen and A. Roy, *Phys. Rev. Lett.* **81**, 4549 (1998); H.B. Chan, V.A. Aksyuk, R.N. Kleiman, D.J. Bishop, and F. Capasso, *Science* **291**, 1941 (2001); R.S. Decca, D. Lopez, E. Fischbach, and D.E. Krause, *Phys. Rev. Lett.* **91**, 050402 (2003).
- [3] The force between a sphere and a plane has been computed for a scalar field with Dirichlet boundary conditions in H. Gies and K. Klingmuller, *Phys. Rev. Lett.* **96**, 220401 (2006); A. Bulgac, P. Magierski, and A. Wirzba, *Phys. Rev. D* **73**, 025007 (2006).
- [4] D.A.R. Dalvit, F.C. Lombardo, F.D. Mazzitelli, and R. Onofrio, *Europhys. Lett.* **68**, 517 (2004).
- [5] M. Brown-Hayes, D.A.R. Dalvit, F.D. Mazzitelli, W.J. Kim, and R. Onofrio, *Phys. Rev. A* **72**, 052102 (2005).
- [6] R. Spero, J.K. Hoskins, R. Newman, J. Pellam, and J. Schultz, *Phys. Rev. Lett.* **44**, 1645 (1980); J. K. Hoskins, R. D. Newman, R. Spero, and J. Schultz, *Phys. Rev. D* **32**, 3084 (1985).
- [7] R. Onofrio, *New J. Phys.* **8**, 237 (2006).
- [8] M. Brown-Hayes, J.H. Brownell, D.A.R. Dalvit, W.J. Kim, A. Lambrecht, F.C. Lombardo, F.D. Mazzitelli, S.M. Middleman, V.V. Nesvizhevsky, R. Onofrio, and S. Reynaud, *J. Phys. A: Math. Gen.* **39**, 6195 (2006).
- [9] A. Ashourvan, M. Miri, and R. Golestanian, *Phys. Rev. Lett.* **98**, 140801 (2007).
- [10] D.A.R. Dalvit, F.C. Lombardo, F.D. Mazzitelli, and R. Onofrio, *Phys. Rev. A* **74**, 020101(R) (2006).
- [11] F.D. Mazzitelli, D.A.R. Dalvit, and F.C. Lombardo, *New J. Phys.* **8**, 240 (2006).
- [12] T. Emig, R.L. Jaffe, M. Kardar, and A. Scardicchio, *Phys. Rev. Lett.* **96**, 080403 (2006); M. Bordag, *Phys. Rev. D* **73**, 125018 (2006).
- [13] F.D. Mazzitelli, M.J. Sánchez, N.N. Scoccola, and J. von Stecher, *Phys. Rev. A* **67**, 013807 (2003).
- [14] E.V. Blagov, G.L. Klimchitskaya, and V.M. Mostepanenko, *Phys. Rev. B* **71**, 235401 (2005).